

Goodput Analysis of NOMA-OTFS Vs NOMA-OFDM under Doubly-Dispersive Channel

Adnan Tariq, Haider Haideri Mehdi, Soo Young Shin

Department of IT Convergence Engineering, Kumoh National Institute of Technology, Gumi.
adnантariq@kumoh.ac.kr, haider_haideri@kumoh.ac.kr, wdragon@kumoh.ac.kr

Abstract

Power-domain non-orthogonal multiple access (PD-NOMA) improves spectral efficiency by superposing multiple users' symbols over the same delay Doppler or time–frequency resources. However, under doubly-dispersive (time and frequency-selective) channels, conventional OFDM experiences inter-carrier interference (ICI) and degraded receiver separation, which directly impacts the reliability and goodput of successive interference cancellation SIC-based NOMA. This paper compares NOMA-OTFS and NOMA-OFDM in a high-mobility doubly-dispersive channel using a BER-driven goodput metric. For a two-user downlink, we sweep the power-difference ΔP and multiple fixed SNR points, report per-user goodput and sum goodput, and discuss the tradeoffs between user separation (SIC robustness) and near-user power starvation.

Keywords: OTFS, OFDM, NOMA, SIC, doubly dispersive channel, goodput, throughput

I. Introduction

NOMA enables multiple users to share the same physical resources by superposition coding and successive interference cancellation (SIC). While NOMA is attractive for high spectral efficiency, its performance depends strongly on (i) channel selectivity, (ii) power allocation (near–far separation), and (iii) SIC error propagation [1]. In high-mobility channels, OFDM suffers from ICI due to Doppler spread, which reduces the effectiveness of equalization and SIC. Orthogonal Time Frequency Space (OTFS) modulation has been proposed as a robust waveform for doubly-dispersive channels by mapping information symbols into the delay–Doppler (DD) domain, where the channel exhibits a structured sparsity [2].

In this work we evaluate goodput (useful delivered rate) rather than raw PHY throughput by incorporating the error rate into the achieved spectral efficiency. The study focuses on a two-user downlink power domain PD-NOMA link and compares NOMA-OTFS and NOMA-OFDM under identical resource configuration and channel conditions.

II. System Model

Let x_1 and x_2 denote the complex data symbols for user-1 (near) and user-2 (far). The transmitted superposed symbol on each resource element is:

$$x = \sqrt{P_1}x_1 + \sqrt{P_2}x_2, \quad P_1 + P_2 = 1, \quad (1)$$

Typically, $P_2 > P_1$ so that the far user is allocated higher power. We parameterize power allocation using the power difference:

$$\Delta P[dB] = 10 \log_{10} \left(\frac{P_2}{P_1} \right), \quad (2)$$

which swept over a predefined range. For each user $u \in \{1,2\}$, let's denote the time-domain transmit vector obtained after applying either OFDM or OTFS modulation (including zero-padding). For user $u \in \{1,2\}$, the received baseband vector is modeled as

$$\mathbf{y}_u = \sqrt{\beta_u} \mathbf{Hs} + \mathbf{w}_u \quad (3)$$

where β_u models large-scale gain (near user stronger, far user weaker), \mathbf{s} is the transmitted time-domain sample vector (obtained from \mathbf{x} through OTFS/OFDM modulation), \mathbf{H} is the doubly-selective channel operator,

capturing delay and Doppler effects (can be seen in [1]), and $\mathbf{w}_u \sim \mathcal{CN}(0, N_0 \mathbf{I})$, where N_0 is the noise variance.

For OFDM-NOMA, a pilot grid is transmitted to estimate the per-resource frequency response using LS estimation, followed by either LMMSE equalization on the composite grid. After demodulation and equalization, each user forms a symbol-domain estimate:

$\mathbf{z}_u = \mathbf{W}_u \mathbf{y}_u = \mathbf{x} + \tilde{\mathbf{w}}_u = \sqrt{P_1} \mathbf{x}_1 + \sqrt{P_2} \mathbf{x}_2 + \tilde{\mathbf{w}}_u$, where \mathbf{W}_u is the equalizer and $\tilde{\mathbf{w}}_u$ is the post-equalization effective noise-plus-residual-interference. For OTFS modulation the receiver uses perfect-CSI time-domain equalization based on the effective OTFS channel matrix \mathbf{G}_u [3]. LMMSE equalization is implemented as

$$\hat{\mathbf{s}}_u = (\mathbf{G}_u^H \mathbf{G}_u + N_0 \mathbf{I})^{-1} \mathbf{G}_u^H \mathbf{y}_u, \quad (4)$$

followed by OTFS demodulation/mapping to obtain \mathbf{z}_u in the grid domain. SIC is applied at the near user by first detecting the far user's higher-power stream from the composite received signal. The far user's symbol is obtained as $\hat{\mathbf{x}}_2 = \mathcal{D} \left(\frac{\mathbf{z}_1}{\sqrt{P_2}} \right)$, reconstructed, and subtracted to form the residual $\mathbf{z}_1^{(1)} = \mathbf{z}_1 - \sqrt{P_2} \hat{\mathbf{x}}_2$. Here, $\mathcal{D}(\cdot)$ denotes the symbol slicer/demapper applied element-wise. The near user then detects its own stream from \mathbf{y}' via $\hat{\mathbf{x}}_1 = \mathcal{D} \left(\frac{\mathbf{z}_1^{(1)}}{\sqrt{P_1}} \right)$. In contrast, the far user performs direct detection without SIC, i.e., $\hat{\mathbf{x}}_2 = \mathcal{D} \left(\frac{\mathbf{z}_2}{\sqrt{P_2}} \right)$, while treating $\sqrt{P_1} \mathbf{x}_1$ as interference. In this work, the SIC decoding order is fixed as $2 \rightarrow 1$.

1. BER-Driven Goodput

Let $k = \log_2(Q)$ denote bits per modulation symbol and $\eta \in (0,1]$ denote an overhead efficiency factor due to cyclic prefix/zero-padding,

$$\eta = \frac{M}{M + \text{padLen}},$$

and the per-user goodput (bps/Hz) is computed as

$$T_u = \eta k (1 - \text{BER}_u), \quad (5)$$

The sum goodput is

$$T_{\text{sum}} = \sum_{u=1}^2 T_u. \quad (6)$$

III. Simulation Setup

In the considered setup, both OTFS and OFDM employ a rectangular resource grid of size $M \times N$, where $M = 32$ denotes the number of subcarriers (delay bins) and $N = 32$ denotes the number of subsymbols (Doppler bins). The subcarrier spacing is set to $\Delta f = 15$ kHz, resulting in a system bandwidth of $BW = M\Delta f = 32 \times 15$ kHz = 0.48 MHz. The carrier frequency is fixed at $f_c = 5$ GHz. Unless otherwise stated, an M -ary modulation is used with baseline 8-PSK and Gray mapping. A high-mobility doubly-dispersive channel is assumed to use the TDL-A [4] multipath profile with user speed $v = 350$ km/h. Large-scale channel gains are modeled as $\beta_{dB} = [0, -8]$ dB, representing a weaker average channel condition for U2.

To study the impact of power allocation, the power-difference parameter is swept over $\Delta P \in \{0, 2, \dots, 20\}$ dB. Performance is evaluated at fixed SNR operating points of $\{10, 20, 30\}$ dB. Under unit-power waveform normalization, the corresponding noise variance is computed as $N_0 = 10^{-SNR(dB)/10}$.

IV. Results and Discussion

Fig. 1 compares the per-user goodput of two-user NOMA-OTFS and NOMA-OFDM versus power difference ΔP at $SNR = \{10, 20, 30\}$ dB. The far user (U2) generally improves with increasing ΔP due to higher allocated power, whereas the near user (U1) exhibits a peaked behavior: small ΔP yields poor SIC, moderate ΔP maximizes U1 goodput, and large ΔP reduces U1 performance due to reduced P_1 . Overall, OTFS provides better per-user goodput around the optimal ΔP , leading to the higher sum goodput observed in Fig. 2.

Fig. 2 shows sum-user goodput trends. In both cases, sum goodput increases with ΔP up to an intermediate optimum and then decreases for large ΔP , reflecting the tradeoff between improved SIC separability and near-user power starvation. NOMA-OTFS consistently achieves a higher peak sum goodput than NOMA-OFDM, with the advantage becoming more evident at higher SNR.

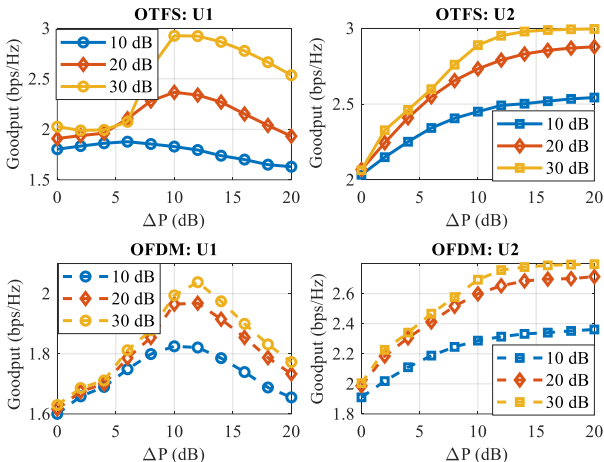


Figure 1: Per-user goodput (U1, U2) vs. ΔP for NOMA-OTFS and NOMA-OFDM at SNR.

V. Conclusion

This paper presented a goodput-based comparison of NOMA-OTFS and NOMA-OFDM under a high-mobility doubly-dispersive channel. Using a two-user downlink PD-NOMA model with SIC at the near user, we computed per-user goodput from measured BER, including overhead efficiency due to padding. The results demonstrate the fundamental tradeoff controlled by ΔP : increasing power separation enhances U2 reliability and SIC feasibility, but excessive separation may starve U1. Under doubly-dispersive conditions, OTFS generally provides improved robustness relative to OFDM, which can translate into goodput gains in relevant $(\Delta P, SNR)$ regions.

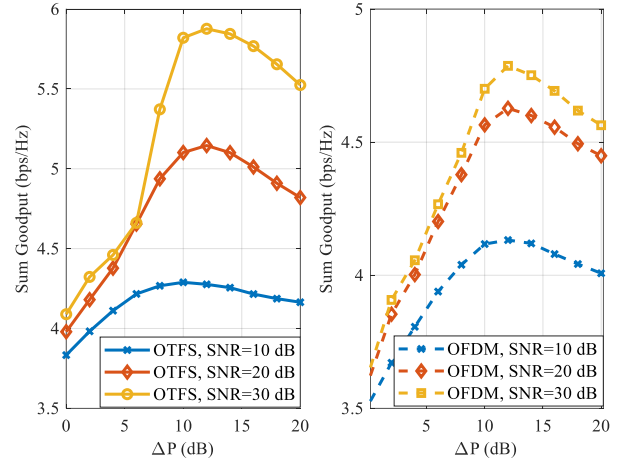


Figure 2: Sum goodput vs. power difference ΔP for NOMA-OTFS and NOMA-OFDM at different SNR values.

Acknowledgment

This work was supported by the National Research Foundation of Korea(NRF) grant funded by the Korea government(MSIT) (RS-2025-00553810, 50%). This work was supported by Innovative Human Resource Development for Local Intellectualization program through the Institute of Information & Communications Technology Planning & Evaluation(IITP) grant funded by the Korea government(MSIT) (IITP-2025-RS-2020-II201612, 50%).

References

- [1] A. Tariq, M. Sajid Sarwar and S. Y. Shin, "Orthogonal Time-Frequency-Space Multiple Access Using Index Modulation and NOMA," in IEEE Wireless Communications Letters, vol. 14, no. 5, pp. 1456-1460, May 2025, doi: 10.1109/LWC.2025.3544234.
- [2] A. Tariq, M. S. Sarwar and S. Young Shin, "Orthogonal Time Frequency Space Index Modulation based on Non-Orthogonal Multiple Access," 2023 14th International Conference on Information and Communication Technology Convergence (ICTC), Jeju Island, Korea, Republic of, 2023, pp. 838-841, doi: 10.1109/ICTC58733.2023.10392492.
- [3] A. Tariq, M.S. Sarwar and S. Y. Shin, "Orthogonal Time Frequency Space (OTFS) with Tri-Mode Index Modulation," 2024 15th International Conference on Information and Communication Technology Convergence (ICTC), Jeju Island, Korea, Republic of, 2024, pp. 1183-1186, doi: 10.1109/ICTC62082.2024.
- [4] 3GPP, "Study on channel model for NR," 3GPP TR 38.901, Version 19.0.0, [12 2025].